

## Ferromagnetism and Antiferromagnetism in 3d Transition Metals

Setsuro ASANO and Jiro YAMASHITA

*Institute for Solid State Physics  
University of Tokyo, Roppongi, Minatoku, Tokyo 106*

(Received September 5, 1972)

The relative stability of ferro- and antiferromagnetic state in 3d transition metals is investigated on the basis of itinerant model, that is, the Stoner model for ferromagnetic states and the gap equation model for antiferromagnetic states. The realistic energy band structures are taken into account and the effective exchange interaction is introduced as only one parameter in the present paper. The theoretical predictions are in good agreement with the observed magnetic diagrams at absolute zero temperature. For example, it is quite reasonable in this model that bcc Fe is ferromagnetic, but fcc Fe is antiferromagnetic. It must be emphasized that there is no need to change the value of effective exchange interaction through all 3d elements to reproduce the observed magnetic moment of them.

### § 1. Introduction

In 1960 Herring wrote an interesting paper entitled "The State of  $d$ -Electrons in Transition Metals".<sup>1)</sup> It seemed to him that the status of the theoretical study of that day was like a variety of different cocktails, in which liquors are mixed according to the taste of each person. Names of four liquors were listed by him: Bands, Correlations, Coupled atoms and Valence bonds, and also four cocktails: Itinerant, Minimum polarity,  $s$ - $d$  Models and Valence. After examining the taste of each cocktail he preferred to "Itinerant" for several reasons, in spite of some shortage inherent to this cocktail. In that article Herring discussed some important problems of the itinerant model being to be studied; for example, self-consistent band calculations, determination of Fermi surfaces and so on. It seems to us that the study of state of  $d$  electrons in transition metals has made a progress along the line he suggested. At present, the itinerant model of transition metals is well founded both theoretically and experimentally, so that the present task is to apply the itinerant model to interpretation of any experimental fact and to examination to what extent it is successful or unsuccessful in each case. Among the many interesting problems in transition metal physics, the problem of relative stability of ferro- and antiferromagnetic state is very interesting. As long as the authors are aware, however, no systematic studies of the problem have been made from the realistic itinerant model which is so successful in the Fermiology.

The purpose of the present paper is to examine the relative stability of ferro-

and antiferromagnetic state in  $3d$  transition metals on the basis of itinerant model. We start with a simple argument. In order to produce some magnetic state from paramagnetic state, there must be some amount of energy loss in the kinetic energy, while there should be some amount of energy gain in the magnetic state owing to effective electron-electron interaction favorable for the parallel spin configuration. The competition of these two factors will determine the stable state. In the present paper, we assume that we are able to evaluate the kinetic energy loss from the energy bands of the Bloch states determined by band calculation. It means that we accept the idea of quasi-particle for  $d$ -electrons in transition metals, and the energy spectrum of quasiparticle is assumed to be well represented by the one obtained by band approximation. The density-of-states of transition metals obtained by the band theory has a complex structure. Some characteristic structures are almost determined by the symmetry of the lattice and some others are proper to the element. It will be shown in the following sections that the structure of the density-of-states (or the joint-density-of-states in the antiferromagnetic case) and the number of conduction electrons (included  $3d$ -electrons) occupying the bands are very important factors to determine the magnetic state. In order to have a systematic picture of the magnetic state of  $3d$  transition metals, it seems necessary to take into account the relative change of  $d$ -band width in each element. (It is not a good approximation to use the same density-of-states curve throughout the  $3d$ -series.) Further, it seems better to use the density-of-states obtained by the coherent potential approximation in order to discuss the magnetic state of alloys of high concentrations. In the present paper, the energy bands in the paramagnetic state are calculated by the Hartree-Fock-Slater self-consistent approximation. The results seem to be quite reasonable. It is probable, however, that other method of calculation gives also a good result, so that the conclusion derived in the present paper will not be restricted to the HFS procedure.

As for the energy gain in the exchange energy due to the induced magnetic moment, we simply assume that it is given by  $-J_{\text{eff}}\delta n^2$ , where  $2\delta n$  is the induced magnetic moment in each atomic site and  $J_{\text{eff}}$  is the effective exchange interaction energy. Since it is difficult to determine  $J_{\text{eff}}$  in the frame of band theory, it is regarded as an adjustable parameter. Once the energy band is given and the amount of energy loss is evaluated as a function of the induced magnetic moment, then the value of  $J_{\text{eff}}$  is easily determined so as to give energy balance at the observed induced magnetic moment. Although  $J_{\text{eff}}$  is a parameter variable from element to element, there is no need to change the value of effective exchange interaction through all  $3d$  elements to reproduce the observed magnetic moment of them. In other words, we find that the Slater-Pauling curve is reproduced from the realistic density-of-states and almost a fixed value of the single parameter  $J_{\text{eff}}$ , and the antiferromagnetic state is predicted as stable at the places in the periodic table really observed. Moreover the value of  $J_{\text{eff}}$  determined is quite small as compared with the value of exchange interaction of bare  $d$ -electrons.

The screening effects seem to be quite effective in transition metals. We have obtained a systematic picture of ferro- and antiferromagnetic state from the band picture. It is true that the real implication of the treatment mentioned here will be clarified only when  $J_{\text{eff}}$  is derived from the first principle. So far we have been concerned only with the absolute zero temperature. The magnetic problem at finite temperature will not be so simple as at absolute zero. If each atom keeps some amount of magnetic moment at finite temperature, the magnetic problem becomes essentially the problem in the disordered lattice, which is not within the power of the simple band theory.

In § 2 the relative stability of the ferro- and antiferromagnetic state with infinitesimal magnetic moment is investigated on the basis of the two non-interacting spin susceptibilities  $\chi_0(\mathbf{0})$  and  $\chi_0(\mathbf{Q})$ . They are evaluated for realistic energy bands of transition metals of bcc and fcc structures. Here  $\mathbf{Q}$  is restricted to  $2\pi/a(001)$ , which corresponds to Cr[Mn]- and  $\gamma$ Mn-type antiferromagnetic state.<sup>2),3)</sup> The theoretical predictions obtained by comparison of  $\chi_0(\mathbf{0})$  and  $\chi_0(\mathbf{Q})$  are found to be in excellent agreement with experimental facts in both fcc and bcc transition metals.

In § 3 the ferro- and antiferromagnetic state with finite magnetic moment are investigated by the Stoner model in ferromagnetism and by the gap equation in antiferromagnetic state. The energy bands of each 3d-transition metal are considered in the form of Mueller's hybridized T.B.-OPW interpolation scheme.<sup>4)</sup> The parameters are determined from the  $E(\mathbf{k})$ -values calculated by the KKR-HFS self-consistent procedure.<sup>5)</sup> It is found that the observed magnetic moments are reasonably explained only when the realistic energy band structures are taken into account. For example, the prediction that bcc Fe is ferromagnetic with about  $2\mu_B$  magnetic moment but fcc Fe is antiferromagnetic with small magnetic moment ( $<1\mu_B$ ) seems to be quite reasonable. The only one parameter in the theory is  $J_{\text{eff}}$  and the value of it is about 0.05~0.06 Ry and there is no need to change the value of this parameter from element to element or according to the situation that it is ferro- or antiferromagnetic state to be considered.

In § 4 iron-based alloys (FeNi, FeCo, FeCr, FeV) are treated by CP approximation and the preliminary results are reported. The Slater-Pauling curve obtained from the rigid band approximation (§ 3) is modified to have much better agreement with experiments, if the alloy effect is taken into account by this approximation.

## § 2. Infinitesimal magnetic moment

Here the relative stability of ferro- and antiferromagnetic state with infinitesimal magnetic moment will be investigated. We start with the non-interacting spin susceptibility<sup>6)</sup>

$$\chi_0(\mathbf{q}) = \frac{4\mu_B^2}{N_A} \sum_{\mathbf{n}'} \sum_{\substack{\mathbf{n}\mathbf{k} \\ \text{occ}}} \frac{|\alpha_{\mathbf{n}\mathbf{k}\mathbf{n}'\mathbf{k}+\mathbf{q}}|^2}{\epsilon_{\mathbf{n}'\mathbf{k}+\mathbf{q}} - \epsilon_{\mathbf{n}\mathbf{k}}}. \quad (1)$$

Here,  $N_A$  is the number of atoms considered and  $\epsilon_{\mathbf{n}\mathbf{k}}$  is the energy eigenvalue of the  $(\mathbf{n}\mathbf{k})$ -Bloch state,  $\phi_{\mathbf{n}\mathbf{k}}$ , and

$$\alpha_{\mathbf{n}\mathbf{k}\mathbf{n}'\mathbf{k}+\mathbf{q}} = \sum_{\mu}' a_{\mathbf{n}\mu}^*(\mathbf{k}) a_{\mathbf{n}'\mu}(\mathbf{k}+\mathbf{q}), \quad (2)$$

where  $a_{\mathbf{n}\mu}(\mathbf{k})$  is the hybridization coefficient of  $\mu$ -orbital of the  $(\mathbf{n}\mathbf{k})$ -Bloch state. The summation  $\sum'$  is restricted to  $d$ -orbitals because, at present, we are interested in the spin susceptibility of  $d$ -orbitals. As is well known, if the condition  $\bar{\chi}_0(\mathbf{q})J_{\text{eff}} > 1$  is satisfied, the non-magnetic state is unstable for the formation of the SDW with wave vector  $\mathbf{q}$  and the optimum wave vector  $\mathbf{q}_0$  is determined by

$$\bar{\chi}_0(\mathbf{q}_0) = \chi_0(\mathbf{q}_0)/2\mu_B^2 = \max. \quad (3)$$

Here  $J_{\text{eff}}$  is the effective exchange interaction between  $d$ -electrons and the effective exchange interaction is assumed to work only when they are on the same atomic site.

The above statement is equivalent to the usual energy consideration; the “ $\langle \text{kinetic energy loss} \rangle + \langle \text{exchange energy gain} \rangle$ ” principle. In our treatment the kinetic energy loss to induce the magnetic moment is estimated as

$$\Delta E_K = \langle M | H_0 | M \rangle - \langle P | H_0 | P \rangle, \quad (4)$$

where  $|P\rangle$  is the wave function of the paramagnetic state,  $|M\rangle$  is that of the magnetic state, which should be determined so as to minimize the kinetic energy loss  $\Delta E_K$  but with the assumed spin polarization, and  $H_0$  is the effective Hamiltonian in the paramagnetic state defined by

$$(H_0 - \epsilon_{\mathbf{n}\mathbf{k}})\phi_{\mathbf{n}\mathbf{k}}(\mathbf{r}) = 0.$$

The assumed spin polarization  $2\delta n_i \mu_B$  at  $i$ -th atomic site contributes to energy gain through exchange term  $\Delta E_{\text{ex}}$ :

$$\begin{aligned} \Delta E_{\text{ex}} &= -\frac{J_{\text{eff}}}{2} \sum_i \{ (n_i + \delta n_i)^2 + (n_i - \delta n_i)^2 \} + \frac{J_{\text{eff}}}{2} \sum_i 2n_i^2 \\ &= -J_{\text{eff}} \sum_i \delta n_i^2. \end{aligned} \quad (5)$$

Then, the net energy gain of magnetic state is written as

$$\Delta E = \Delta E_K - J_{\text{eff}} \sum_i \delta n_i^2. \quad (6)$$

(It is assumed that there is no charge density wave in magnetic state.)

The loss in the kinetic energy to induce the infinitesimal magnetic moment,  $2\delta n \cos(\mathbf{q}\mathbf{R}_i)$ , at each atomic site is evaluated by the second-order perturbation as

$$\Delta E_K = \frac{N_A}{2\bar{\chi}_0(\mathbf{q})} \delta n^2 + O(\delta n^4), \quad (7)$$

so that the net energy gain is given by

$$\Delta E = \frac{N_A}{2} \left( \frac{1}{\bar{\chi}_0(\mathbf{q})} - J_{\text{eff}} \right) \delta n^2. \quad (8)$$

If  $J_{\text{eff}}\bar{\chi}_0(\mathbf{q}) > 1$ , the non-magnetic state becomes unstable, because the exchange energy gain exceeds the kinetic energy loss. It also means that, if  $\bar{\chi}_0(\mathbf{0}) > \bar{\chi}_0(\mathbf{q})$  for any wave vector  $\mathbf{q}$ , the ferromagnetic state is stable and, if  $\bar{\chi}_0(\mathbf{q}) > \bar{\chi}_0(\mathbf{0})$ , the antiferromagnetic state is stable. The latter takes place, simply because the magnetic moment is induced with less kinetic energy loss.

It is desirable to calculate  $\bar{\chi}_0(\mathbf{q})$  for all  $\mathbf{q}$  and determine the optimum  $\mathbf{q}$  value for each transition metal, but this is very elaborate work. In this paper  $\mathbf{q}$  is restricted to  $\mathbf{Q} = 2\pi/a(001)$ , which corresponds to the Cr[Mn]- and  $\gamma$ Mn-type antiferromagnetic state, and the relative stability of magnetic states is investigated. As is well known,  $\bar{\chi}_0(\mathbf{0})$  is reduced to the density of states ( $d$ -states in the case of Eq. (1)) at the Fermi surface, and  $\bar{\chi}_0(\mathbf{Q})$  is directly calculated by Eq. (1). Mueller's hybridized T.B.-OPW interpolation scheme<sup>4)</sup> is very convenient for such calculation. In practice,  $E(\mathbf{k})$ -values and wave functions of 505 and 506 non-equivalent  $\mathbf{k}$ -points in 1/48 B.Z. are used for fcc and bcc structure, respectively. (Some cares are taken to avoid the statistical error in performing the summation in  $\mathbf{k}$ -space.) Mueller's interpolation parameters are determined from the  $E(\mathbf{k})$ -values of bcc Cr and fcc Mn, which are calculated by KKR-HFS self-consistent procedure with  $\lambda = 0.8$ .<sup>5)</sup> The calculated  $\bar{\chi}_0(\mathbf{0})$  and  $\bar{\chi}_0(\mathbf{Q})$  are shown in Fig. 1 for bcc and fcc transition metals as a function of the number of valence electrons  $N$  (the number of 3d- and 4s-electrons).

In the case of bcc structure (Fig. 1(a)) there is a sharp peak in  $\bar{\chi}_0(\mathbf{Q})$  near Cr, which obviously reflects the characteristic structure of the Fermi surface of Cr. The peak exists at  $N = 6.1$ , which means that the perfect antiferromagnetic state is probably most favorable around  $N = 6.1$ . Corresponding to this situation, experiments show that pure Cr ( $N = 6.0$ ) has a sinusoidal SDW state with wave vector  $\mathbf{q} = 2\pi/a(0, 0, 0.95)$ , which is a little smaller than  $\mathbf{Q}$  and, when a small amount of Mn or Re is added ( $N > 6.0$ ), the perfect antiferromagnetic state with wave vector  $\mathbf{Q}$  is realized.<sup>7)</sup> Comparison of  $\bar{\chi}_0(\mathbf{0})$  and  $\bar{\chi}_0(\mathbf{Q})$  in Fig. 1(a) predicts that, in bcc structure, when  $N < 6.6$  the antiferromagnetic state is stable and when  $N > 6.6$  the ferromagnetic state is stable, which is in good agreement with experimental facts.<sup>8), 9)</sup> (Fig. 5.)

In fcc structure various transition metal alloys show the 'inver effect' and the spontaneous magnetization suddenly drops down near  $N = 8.5$ .<sup>9)</sup> (Fig. 5.) Ferromagnetism in fcc transition metals, therefore, seems to be stable only at  $N \geq 8.5$ . On the other hand,  $\gamma$ Mn and  $\gamma$ Fe seem to be antiferromagnetic.<sup>10)</sup> Various fcc alloys with  $7.0 < N < 8.0$  also show the antiferromagnetic structure, which

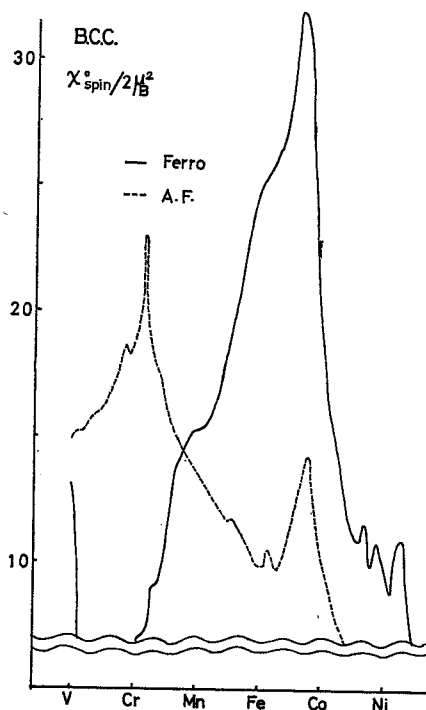


Fig. 1(a). Non-interacting spin susceptibility of bcc transition metals. The ferromagnetic one ( $\bar{\chi}_0(0)$ ) is shown by the solid line and the antiferromagnetic one ( $\bar{\chi}_0(Q)$ ) is shown by the dotted line. They are evaluated by Mueller's interpolation scheme adopting the energy bands of Cr.

mentioned above are just what Fig. 1(b) tells us. Thus, the theoretical prediction through comparison of  $\bar{\chi}_0(0)$  and  $\bar{\chi}_0(Q)$  agrees excellently well with the experiments.

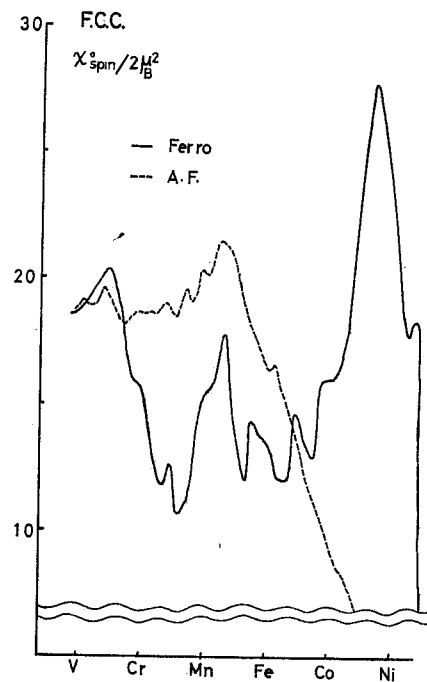


Fig. 1(b). Those of fcc transition metals. The energy bands of fcc Mn are used.

is confirmed by neutron diffraction experiments.<sup>11)</sup> Some fcc alloys with  $8.0 < N < 8.5$  also seem to be antiferromagnetic. The experimental situations

### § 3. Finite magnetic moment

In this section let us investigate the magnetic state with finite magnetic moment following the assumption that the net energy gain in magnetic state is given by Eq. (6); the  $\langle \text{kinetic energy loss} \rangle + \langle \text{exchange energy gain} \rangle$ . Then the magnitude of the induced magnetic moment is determined from the condition

$$\frac{\partial \Delta E}{\partial \delta n} = 0.$$

In the ferromagnetic state the loss in the kinetic energy to induce the magnetic moment  $2\delta n\mu_B$  in each atomic site is given by

$$\Delta E_K = \int_{\mu}^{\mu^+} \epsilon \rho(\epsilon) d\epsilon - \int_{\mu^-}^{\mu} \epsilon \rho(\epsilon) d\epsilon, \quad (9)$$

where

$$\delta n = \int_{\mu}^{\mu^+} \rho(\epsilon) d\epsilon - \int_{\mu^-}^{\mu} \rho(\epsilon) d\epsilon \quad (10)$$

and  $\rho(\epsilon)$  is the density of states per single spin and  $\mu$  is the Fermi energy in the paramagnetic state. Then, the net energy gain is given by

$$\Delta E = \Delta E_K - J_{\text{eff}} \delta n^2.$$

The energy minimum condition gives the equation

$$\mu^+ - \mu^- = 2J_{\text{eff}} \delta n, \quad (11)$$

which should be solved self-consistently with Eq. (10). Thus, in the ferromagnetic case the induced magnetic moment is easily determined by the Stoner condition only if the density-of-states curve in the paramagnetic state is known.

In the antiferromagnetic case the same gap equation as given below can be derived from the energy minimum condition, but in this paper it is derived in an intuitive way.

In the antiferromagnetic state itinerant electrons feel the lower potential at the same spin site and the higher potential at the opposite spin site because of the exchange interaction. Then, the electrons are apt to concentrate on the same spin site rather than on the opposite spin site, so that the state of the net spin polarization comes out. As the resultant spin polarization should make up the assumed exchange potential, the spin polarization and the exchange potential should be determined self-consistently. This self-consistent equation can be easily solved in the hybridized T.B.-OPW model. First we assume that electrons feel the lower exchange potential by  $-g$  at the same spin-site and the higher exchange potential by  $+g$  at the opposite spin site. Then the polarized spin charge  $2\delta n$  is easily evaluated as a function of  $g$  and  $N$  (Eq. (3.5) in Ref. 3)), where  $N$  is the number of  $3d$  and  $4s$  valence electrons. As the resultant spin polarization must make up the assumed exchange potential, the self-consistent gap equation is written as

$$g = J_{\text{eff}} \delta n(g, N), \quad (12)$$

if we assume the same type of effective exchange interaction as in Eq. (5). In the practical calculation, Mueller's combined interpolation scheme (hybridized T.B.-OPW model) is adopted and  $g$  is taken as off-diagonal matrix element between  $\{\mathbf{k}\}$  and  $\{\mathbf{k}+\mathbf{q}\}$   $d$ -state. Here, the effective exchange interaction is assumed to work only between  $d$ -states. Details were shown in the previous paper.<sup>3)</sup>

To perform the above calculation we must know the energy bands of each transition metals in the paramagnetic state. Here they are determined by the KKR-HFS self-consistent procedure, but the original Slater exchange is reduced

Table I. The calculated  $E(k)$ -values of several symmetrical points for fcc Cu, Ni, Co, Fe, Mn and for bcc Fe, Mn, Cr, V, Ti. They are determined by the KKR-HFS self-consistent procedure with  $\lambda=0.8$ .<sup>5)</sup> Here  $s$ ,  $p$  and  $d$  denote the self-consistent electronic charge with  $s$ -,  $p$ - and  $d$ -symmetry within the inscribed sphere. r.m.s. is the r.m.s. error of Mueller's interpolation scheme. The lattice constant  $a$  is given in atomic unit and the energy is given in Ry unit.  $E(\Gamma'_{25})$  is taken as energy standard.

fcc structure

	Cu	Ni	Co	Fe	Mn
$a$	6.822	6.652	6.709	6.784	6.983
$\Gamma_1$	-.394	-.461	-.455	-.448	-.439
$\Gamma'_{25}$	.000	.000	.000	.000	.000
$\Gamma_{12}$	.054	.072	.079	.086	.088
$X_1$	-.128	-.176	-.190	-.204	-.209
$X_5$	.105	.139	.153	.167	.171
$L'_2$	.208	.163	.157	.152	.132
$s$	.498	.440	.433	.428	.430
$p$	.438	.392	.404	.415	.425
$d$	9.445	8.503	7.457	6.413	5.390
rms	—	.0064	.0066	.0067	.0070

bcc structure

	Fe	Mn	Cr	V	Ti
$a$	5.424	5.424	5.442	5.745	6.255
$\Gamma_1$	-.447	-.451	-.457	-.456	-.455
$\Gamma'_{25}$	.000	.000	.000	.000	.000
$\Gamma_{12}$	.097	.111	.126	.120	.104
$H_{12}$	-.176	-.205	-.238	-.232	-.208
$H'_{25}$	.164	.189	.219	.210	.185
$N'_1$	.183	.182	.178	.122	.042
$s$	.384	.375	.363	.377	.408
$p$	.355	.370	.379	.355	.321
$d$	6.363	5.295	4.251	3.286	2.374
rms	.0078	.0096	.0111	—	—

by factor 0.8.<sup>5)</sup> The calculated  $E(k)$  values for several symmetrical points are given in Table I for bcc V, Cr, Mn, Fe and for fcc Mn, Fe, Co, Ni, Cu. In order to have a quick view, we define the width of  $d$ -bands as

$$W_d = E(H'_{25}) - E(H_{12}) \quad \text{for bcc}$$

$$= E(X_5) - E(X_1) \quad \text{for fcc}$$

and the separation of  $sp$ - and  $d$ -bands as

$$W_{sd} = \frac{1}{5}(3E(\Gamma'_{25}) + 2E(\Gamma_{12})) - E(\Gamma_1).$$

The results are shown in Fig. 2. The  $d$ -band width becomes wider from Cu to



Cr and it takes a maximum value around Cr.

Next the calculated  $E(\mathbf{k})$ -values are represented by Mueller's combined interpolation scheme. For fcc transition metals original Mueller's method reproduces the  $E(\mathbf{k})$ -values very well. (The r.m.s. error  $\sim 0.006$  Ry.) But for bcc transition metals the straightforward extension to bcc structure is not so good and some modification is necessary.<sup>\*)</sup> The r.m.s. error in the fitting of  $E(\mathbf{k})$ -values are given in Table I.

After these procedures the magnetic moments in each transition metals are determined from the hybridized T.B.-OPW model. In the ferromagnetic case Eq. (11) is solved self-consistently with Eq. (10). In the antiferromagnetic case the self-consistent gap equation is solved as mentioned before. The value of  $J_{\text{eff}}$ , which is the only parameter here, is chosen so as to give the observed spin polarization, but it is not adjusted so as to give the observed value exactly, because there may be some other contributions, angular momentum contribution or polarization of  $s$ -electrons, etc.

The results of calculation are shown in Fig. 3(a) for fcc transition metals. The energy bands of fcc Ni, Co, Fe and Mn are used in the vicinity of each transition metal. As mentioned previously, the density-of-states of fcc transition metals has a sharp peak at the top of  $d$ -bands,<sup>13)</sup> which stabilizes the ferromagnetic state in fcc Ni and Co. This peak is so sharp that it exists narrowly only between Co and Ni. (The ferromagnetic spin susceptibility  $\bar{\chi}_0(0)$  in Fig. 1(b) roughly shows the density-of-states curve in fcc structure.) Thus, if the value of  $J_{\text{eff}}$  is suitably chosen, the condition  $J_{\text{eff}}\bar{\chi}_0(0) > 1$  is satisfied only between Co and Ni. Then, the paramagnetic state becomes stable for infinitesimal ferromagnetic state, when the valence electron number is reduced from Co ( $N=9.0$ ). The situation is different for the ferromagnetic state with finite magnetic moment. The sharp peak at the top of  $d$ -bands of the majority spin is fully occupied in the ferromagnetic state, so that it has energy lower than the paramagnetic state, so long as  $N$  is not reduced beyond some critical value  $N_c$ . At  $N_c$  the energy of paramagnetic state is equal to that of strong ferromagnetic state and the spontaneous magnetization suddenly disappears probably by first-order transition. Experimentally fcc transition metal alloy shows 'inver effect' near  $N=8.5$  (Fig. 5) and the spontaneous magnetization suddenly drops down there. In our model the

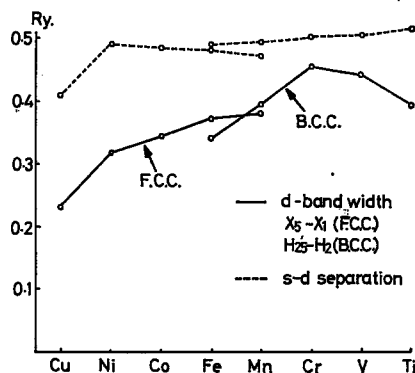


Fig. 2. Comparison of  $d$ -band width and  $s$ - $d$  separation in 3d transition metals. They are evaluated by the KKR-HFS self-consistent procedure with  $\lambda=0.8$ .<sup>5)</sup>

\*) For bcc structure seven plane waves (000), (-200), (-1-10), (-10-1), (-110), (-101) and (0-1-1) are used. The  $s$ - $d$  hybridization term and the non-orthogonal term ( $g$  and  $f$  in Mueller's paper) are distinguished between  $d\epsilon$  and  $d\gamma$  states and they are cut off more sharply than Mueller's.

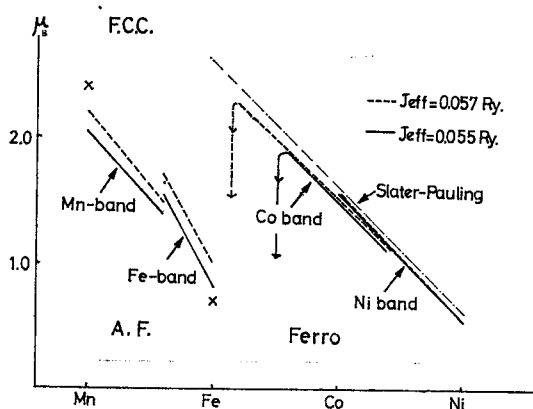


Fig. 3(a). The induced magnetic moment in  $3d$ -transition metals for ferro- and antiferromagnetic states. They are determined by the self-consistent procedure mentioned in the text, taking into account the realistic energy band structures for each transition metal.

In § 2 the comparison of  $\bar{\chi}_0(0)$  and  $\bar{\chi}_0(Q)$  predicts that antiferromagnetic state is stable at  $N < 8.5$ . The gap equation (12) is solved for  $Q = 2\pi/a(001)$  with  $J_{\text{eff}} = 0.055$  Ry between Mn and Fe ( $7.0 \leq N \leq 8.0$ ). The calculated magnetic moment of  $\gamma\text{Fe}$  is  $0.8\mu_B$ , where the energy band of  $\gamma\text{Fe}$  is used, and that of  $\gamma\text{Mn}$  is  $2.0\mu_B$ , where the energy band of  $\gamma\text{Mn}$  is used. The corresponding observed values are  $0.7\mu_B$  and  $2.4\mu_B$ .<sup>10)</sup> Agreement seems to be satisfactory. In our model the antiferromagnetic state is probably stable in some extended region at  $N < 7.0$ , but it is not stable at  $N \geq 8.1$ . Therefore, it might be concluded that at  $8.1 < N < 8.5$  the paramagnetic state or the antiferromagnetic state with more complex spin structure is stable. But it must be noted that the model is essentially a rigid-band model, and it is rather questionable to apply this model to such a critical problem.

In Fig. 3(b) the calculated results are shown for bcc transition metals. In the ferromagnetic state the energy band of bcc Fe is used and in the antiferromagnetic state that of bcc Cr is used. If the value of  $J_{\text{eff}}$  is taken as 0.051 Ry, the observed magnetic moment  $2.2\mu_B$  is obtained for bcc Fe. The over-all structure of Slater-Pauling curve seems to be explained by the rigid-band model. For example, bcc Fe has a weak ferromagnetic state, where  $d$ -bands of majority spin state are not fully occupied, and the mean magnetic moment  $\langle\mu\rangle$  has a maximum between Fe and Co, but at  $N < 8.0$ ,  $\langle\mu\rangle$  is not decreased linearly like experiments.

It will be shown in § 4 that this discrepancy is really improved, if we take into account the alloy effect by CP approximation. The antiferromagnetic state with  $Q = 2\pi/a(001)$  in bcc structure is predicted near Cr, but the predicted magnetic moment is very sensitive to the choice of  $J_{\text{eff}}$ . If we choose  $J_{\text{eff}}$  as

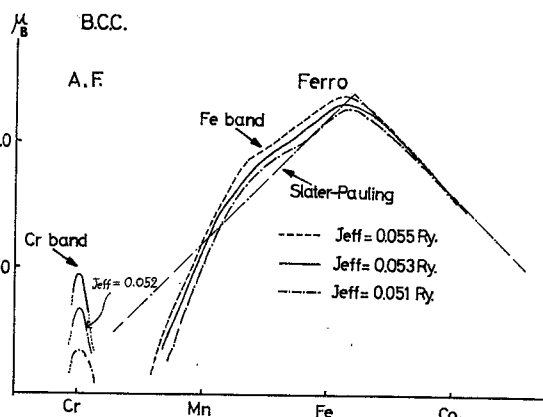


Fig. 3(b). The same figure for bcc structure.

critical value  $N_c$  is very sensitive to the choice of  $J_{\text{eff}}$  and  $J_{\text{eff}}$  is estimated as 0.055 Ry if we assume that  $N_c = 8.5$ .

0.052 Ry, the observed magnetic moment is just predicted, but the region of its stable existence is very narrow around  $N=6.1$ , where  $\chi_0(Q)$  has a sharp maximum and the CsCl type antiferromagnetic state is expected to be most stable.

Experimentally the mean magnetic moment and the Néel temperature of  $\text{Cr}_{1-x}\text{Re}_x$  alloy have a maximum around  $x=0.05\sim 0.10$  ( $N=6.05\sim 6.10$ ) and the region of the stable existence of antiferromagnetic state is restricted to  $6.0\lesssim N\lesssim 6.2$ , where the experimental curve is quite similar to the calculated magnetization curve in Fig. 3(b).<sup>13)</sup> The observed specific heat of antiferromagnetic  $\text{Cr}_{1-x}\text{Re}_x$  alloy also seems to have a minimum around  $N\approx 6.1$ <sup>14)</sup> and supports the view that the nesting effect is most effective around  $N=6.1$ . Therefore, in  $\text{Cr}[\text{Re}]$  alloy the rigid-band approximation seems to be rather good and the calculated results in Fig. 3(b) seem to have some correspondence with experiments.  $\text{CrMn}$  alloy, however, is antiferromagnetic at  $6.0<N\lesssim 6.5$  and the mean magnetic moment and the Néel temperature increases monotonically with  $N$ , which contradicts our present calculation. Probably in  $\text{CrMn}$  alloy the rigid-band model or the assumption of constant  $J_{\text{eff}}$  breaks down. On the other hand, if we use the energy band of bcc Mn and assume  $J_{\text{eff}}\approx 0.053$  Ry, the induced magnetic moment in the antiferromagnetic state is estimated as about  $1\mu_B$  at  $N\approx 6.4$ . Thus the results seem to be so sensitive as to give a reliable conclusion, but it is probable that  $J_{\text{eff}}$  is a little larger in Mn-site than in Cr-site. It should be noted that the rigid-band model cannot explain the induced magnetic moment of concentrated  $\gamma\text{FeMn}$  alloy.<sup>9)</sup>

Another example clearly shows that energy band of bcc transition metal has a CsCl type instability just around  $N=6.1$ . Nevitt<sup>15)</sup> investigated extensively the CsCl type super-lattice and found that the transition metal alloys, such as VMn, TiFe or ScCo, in which the valence electron number per atom is 6.0, like CsCl type super-structure. Probably, some of them are stabilized by a mechanism similar to the antiferromagnetic state in  $\text{Cr}[\text{Mn}]$ .<sup>16)</sup> One of the typical examples may be FeCo super-lattice. The mean valence electron number of FeCo alloy is 8.5 per atom. But this alloy is ferromagnetic with  $4.8\mu_B$  per unit cell. The mean valence electron number in minority spin, therefore, is just 6.1 per unit cell and the above mechanism effectively stabilizes the CsCl structure in the minority spin state.

In conclusion, if the realistic energy band structures are taken into account, the observed magnetic diagrams of 3d-transition metals at null temperature are reasonably explained with only one parameter  $J_{\text{eff}}$ , which seems to be almost constant in ferromagnetic and antiferromagnetic states both for fcc and bcc transition metals. In other words, the ferromagnetic state is realized, when the energy bands have high density-of-states, and the antiferromagnetic state is realized when the energy bands tend to split by the perturbation which produces the magnetic super-lattice. In fcc structure the density-of-states curve has a very

sharp peak at the top of  $d$ -bands, and the energy bands tend to split near  $N \approx 7.3$  (Fig. 1(b)). Therefore the ferromagnetic state is stable only at Co and Ni, and fcc Mn and fcc Fe are antiferromagnetic. In bcc structure, the density-of-states curve has a rather broad peak just near  $\text{Fe}^{17)}$  and the energy bands split at  $N=6.1$ . Therefore bcc Fe is ferromagnetic and bcc Cr[Mn] is antiferromagnetic.

At present we cannot answer the question why  $J_{\text{eff}}$  is so constant, because the problem of electron correlation in transition metals is not yet well understood. The fact which seems to be reliable is that in transition metals the correlation effect reduces the exchange interaction very much and probably five times of  $J_{\text{eff}}$  cannot exceed the  $d$ -band width.<sup>18)</sup> Therefore, the fact that the effective exchange interaction ( $J_{\text{eff}}$ ) does not depend on the transition metal elements or the kind of magnetic state is only a matter of analysis of the experiments in a reasonable way. Here it should be noticed that constancy of  $J_{\text{eff}}$  is derived only when we use the self-consistent energy bands for each transition metal. If the rigid-band model is used for all transition metals the value of  $J_{\text{eff}}$ , which gives the observed magnetic moment, is not so constant. For example, if we use the energy bands of bcc Cr instead of those of bcc Fe, the value  $J_{\text{eff}}=0.068$  Ry is necessary to induce the observed magnetic moment  $2.2\mu_B$ . This is simply because the  $d$ -band width of bcc Cr is about 34% wider than that of bcc Fe, and the wider bands need the larger loss in kinetic energy and the larger value of  $J_{\text{eff}}$  by about 34% to induce the magnetic moment of the same magnitude. In this way the choice of  $J_{\text{eff}}$  is deeply related to the  $d$ -band width and, hence, to the choice of effective potentials of paramagnetic state. If another self-consistent procedure is adopted, another set of  $J_{\text{eff}}$  may be obtained to explain the observed magnetic diagrams. But in each set of  $J_{\text{eff}}$ , the value is expected to be rather constant from element to element. This is because the absolute value of the  $d$ -band width may be somewhat dependent on the method of the self-consistent procedure, but the relative value of  $d$ -band width is expected to be rather independent of the methods so long as the self-consistent procedure, at least in the Coulomb potential, is adopted. In our experience, if the KKR-HFS self-consistent procedure with  $\lambda=2/3$  is adopted,<sup>6)</sup>  $J_{\text{eff}}$  must be increased by 8% for all elements. Therefore, the absolute value of  $J_{\text{eff}}$  should not be taken so seriously.

Finally we note that some experiments about the exchange energy splitting support or, at least, do not contradict our present calculations. Recently magnetic energy gap in antiferromagnetic Cr[Mn] alloy is observed by the optical absorption. The observed value is about 0.36 eV in the perfect antiferromagnetic state with  $Q=2\pi/a(001)$ .<sup>19)</sup> In our model it is estimated as  $2J_{\text{eff}}\delta n \approx 0.42$  eV for  $2\delta n=0.6\mu_B$ . In ferromagnetic hcp-Co, the exchange splitting is estimated as 1.1 eV from the photoemission data.<sup>20)</sup> In our model it is estimated as  $2J_{\text{eff}}\delta n \approx 1.1 \sim 1.2$  eV. In ferromagnetic Ni, Phillips estimated the exchange splitting as  $0.5 \pm 0.1$  eV,<sup>21)</sup> where the corresponding value is about 0.4 eV in our model.

#### § 4. Magnetic moments of Fe-based alloy by CP approximation

In the previous section the rigid-band approximation is assumed and the fluctuation of the potential at each atomic site is not taken into account. In the ferromagnetic state this is easily taken into account by the CP approximation.<sup>22)</sup> In this section the preliminary results for Fe-based alloy are presented. The model is the same as that developed by Kirkpatrick et al.<sup>28)</sup> The density-of-states of pure bcc Fe in § 3 is used as the base. The atomic  $d$ -levels are determined as follows:

$$\varepsilon_A^\pm = \varepsilon_A^0 + U_A(n_A - n_A^0) \mp J_{\text{eff}}\delta n_A, \quad (13)$$

$$\varepsilon_B^\pm = \varepsilon_B^0 + U_B(n_B - n_B^0) \mp J_{\text{eff}}\delta n_B, \quad (14)$$

$$n_A = n_A^+ + n_A^-,$$

$$n_B = n_B^+ + n_B^-,$$

$$2\delta n_A = n_A^+ - n_A^-,$$

$$2\delta n_B = n_B^+ - n_B^-.$$

Here  $A$  and  $B$  specify the kind of atoms and  $+$  and  $-$  specify the majority and minority spin state at each atomic site, respectively.  $n_A^\pm$  ( $n_B^\pm$ ) denotes the occupation number of  $d$ -orbitals in each spin state of  $A$  ( $B$ ) atomic site. Hence  $2\delta n_A$  or  $2\delta n_B$  are the induced magnetic moment of  $A$  or  $B$  atom.  $n_A^0$  ( $n_B^0$ ) is the occupation number of  $d$ -orbitals in pure states and  $\varepsilon_A^0$  ( $\varepsilon_B^0$ ) is the atomic  $d$ -levels with  $n_A = n_A^0$  ( $n_B = n_B^0$ ). They are estimated from the band calculation in § 3.  $U_A$  ( $U_B$ ) is the intra-atomic Coulomb interaction between  $d$ -orbitals and calculated from  $d$ -wave functions of free atoms and  $J_{\text{eff}}$  is the effective exchange interaction mentioned before. The adopted values are shown in Table II.

Once the spin-dependent atomic  $d$ -levels,  $\varepsilon_A^\pm$  and  $\varepsilon_B^\pm$  are given, the occupation number of each atomic site,  $n_A^\pm$  and  $n_B^\pm$ , are determined by applying the CP approximation for majority and minority spin bands separately and by integrating the local density of states.<sup>28)</sup> Fermi energy is determined from the condition

$$c_A n_A + c_B n_B = c_A n_A^0 + c_B n_B^0,$$

where  $c_A$  ( $c_B$ ) is the concentration of  $A$  ( $B$ ) atoms. In our calculation, therefore, the  $sp$ -states are assumed to be rigid and only the  $d$ -states are treated by

Table II. Parameters used for the calculation of Fe-based alloy.

	$n^0/2$	$\varepsilon^0$ (Ry)	$U$ (Ry)
V	1.98	-.021	1.40
Cr	2.51	-.041	1.52
Fe	3.49	-.184	1.73
Co	3.98	-.205	1.83
Ni	4.46	-.234	1.93

CP approximation. The resultant  $n_A^\pm$  and  $n_B^\pm$ , on the other hand, must satisfy Eqs. (13) and (14). Thus,  $\epsilon_A^\pm$ ,  $\epsilon_B^\pm$ ,  $n_A^\pm$  and  $n_B^\pm$  and, hence, the induced magnetic moment  $2\delta n_A$  and  $2\delta n_B$  should be determined self-consistently for assumed value of  $J_{\text{eff}}$ .

The mean magnetic moment ( $2c_A\delta n_A + 2c_B\delta n_B$ ) is calculated for several Fe-based alloys by a self-consistent procedure and the result is shown in Fig. 4. For FeCo and FeNi alloys the results are stable for the choice of  $J_{\text{eff}}$ , but for FeCr, in which the  $d$ -bands in majority spin are partially occupied, the results are very sensitive to the choice of  $J_{\text{eff}}$ . If we choose  $J_{\text{eff}} = 0.051$  Ry for both Fe and Cr site, the induced magnetic moment at Cr site becomes negative to excess and the mean magnetic moment is reduced also excessively with increasing concentration of Cr. As mentioned in the previous section, in the pure states the value of  $J_{\text{eff}}$  to induce the magnetic moment of the same magnitude is almost proportional to the  $d$ -band width,  $W_d$ . As seen from Fig. 2, the  $d$ -band width of Cr is about 34% wider than that of Fe. In this case, this difference should be taken into account as the randomness of transfer matrix element, but it is a troublesome work. In this paper it is effectively taken into account by distinguishing the effective exchange interaction in each atomic site and assuming that

$$\frac{J_{\text{eff}}^A}{W_d^A} = \frac{J_{\text{eff}}^B}{W_d^B}. \quad (15)$$

The results are shown by the solid line in Fig. 4. Comparing them with the experimental results in Fig. 5<sup>9)</sup> we find that the agreement seems to be good in qualitative sense. It is noticeable that the qualitative difference between FeCr and FeV alloys revealed in experiments is also shown in the calculated results.

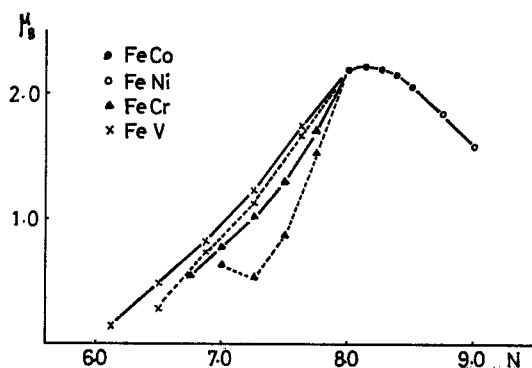


Fig. 4. The mean magnetic moment in Fe-based bcc alloys calculated by CP approximation. The solid line shows the case in which  $J_{\text{eff}}$  is distinguished in two kinds of atomic sites assuming Eq. (15). The dotted line shows the case in which  $J_{\text{eff}}$  is assumed to be the same in both Fe and Cr(V) sites.

It is, however, not satisfactory in quantitative sense because experiments show that the mean magnetic moment in FeCo alloy is more increased near

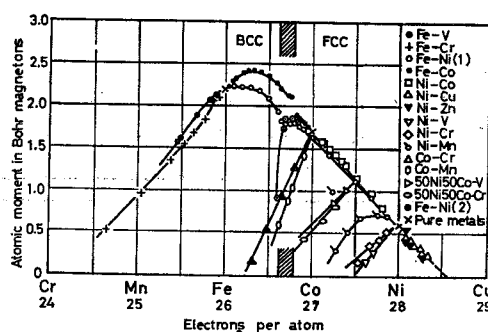


Fig. 5. The mean magnetic moment observed in bcc and fcc ferromagnetic alloy (Ref. 9)).

$N=8.1$  and that the mean magnetic moments are reduced more slowly in FeCr and FeV alloys.

In Fig. 6 the calculated magnetic moments for each atomic site are shown for FeCr alloy and compared with neutron diffraction experiments.<sup>24)</sup> Qualitatively the agreement is satisfactory. Quantitatively, however, the negative polarization in Cr is a little larger, even if the difference in the band width is considered by the assumption of Eq. (15). Anyhow, the Slater-Pauling curve in Fig. 3(b) derived by rigid-band approximation is much improved if the alloy effect is taken into account by CP approximation.

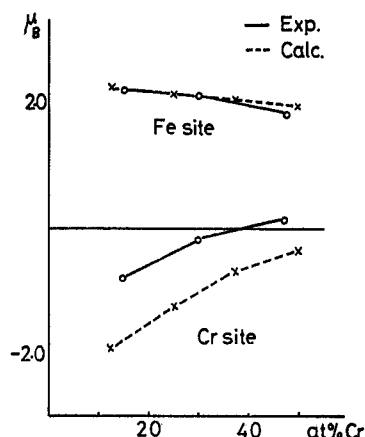


Fig. 6. The induced magnetic moment in each atomic site of FeCr alloy.  $J_{\text{eff}}$  is chosen as Eq. (15).

#### References

- 1) C. Herring, J. Appl. Phys. Suppl. **31** (1960), 3S.
- 2) W. M. Lomer, Proc. Phys. Soc. **80** (1962), 489.  
S. Asano and J. Yamashita, J. Phys. Soc. Japan **23** (1967), 714.
- 3) S. Asano and J. Yamashita, J. Phys. Soc. Japan **31** (1971), 1000.
- 4) F. M. Mueller, Phys. Rev. **153** (1967), 659.
- 5) S. Asano and J. Yamashita, J. Phys. Soc. Japan **30** (1971), 667.
- 6) P. Lederer and A. Blandin, Phil. Mag. **14** (1966), 363.
- 7) W. C. Koehler, R. M. Moon, A. L. Trego and A. R. Mackintosh, Phys. Rev. **151** (1966), 405.
- 8) Y. Hamaguchi and N. Kunitomi, J. Phys. Soc. Japan **19** (1964), 1849.
- 9) S. Chikazumi, *Physics of Magnetism* (John Wiley & Sons, Inc., 1964), p. 73.
- 10) G. E. Bacon, I. W. Dunmur, J. H. Smith and R. Street, Proc. Roy. Soc. **A241** (1957), 223.  
S. C. Abrahams, L. Guttman and J. C. Kasper, Phys. Rev. **127** (1962), 2052.
- 11) Y. Endoh and Y. Ishikawa, J. Phys. Soc. Japan **30** (1971), 1614.
- 12) J. W. D. Connolly, Phys. Rev. **159** (1967), 415.
- 13) A. L. Trego and A. R. Mackintosh, Phys. Rev. **166** (1968), 495.
- 14) F. Heiniger, Phys. Kondens. Materie **5** (1966), 285.
- 15) M. V. Nevitt, *Electronic Structure and Alloy Chemistry of the Transition Elements*, ed. by P. A. Beck (John Wiley & Sons, 1963), p. 101.
- 16) J. Yamashita and S. Asano, Prog. Theor. Phys. **48** (1972), 2119.
- 17) S. Wakoh and J. Yamashita, J. Phys. Soc. Japan **21** (1966), 1712.
- 18) J. Kanamori, Prog. Theor. Phys. **30** (1963), 275.
- 19) L. W. Bos and D. W. Lynch, Phys. Rev. **B2** (1970), 4567.
- 20) S. Wakoh and J. Yamashita, J. Phys. Soc. Japan **28** (1970), 1151.
- 21) J. C. Phillips, J. Appl. Phys. **39** (1968), 755.
- 22) H. Hasegawa and J. Kanamori, J. Phys. Soc. Japan **31** (1971), 382.
- 23) S. Kirkpatrick, B. Velický and H. Ehrenreich, Phys. Rev. **B1** (1970), 3250.
- 24) C. G. Shull and M. K. Wilkinson, Phys. Rev. **97** (1955), 304.